The Activation Mechanism of Ru–Indenylidene Complexes in Olefin Metathesis

César A. Urbina-Blanco,[†] Albert Poater,[§] Tomas Lebl,[†] Simone Manzini,[†] Alexandra M. Z. Slawin,[†] Luigi Cavallo,*[‡,‖] and Steven P. Nolan*[†]

[†]EaStCHEM School of Chemistry, University of St. Andrews, North Haugh, St. Andrews, Fife, KY16 9ST, United Kingdom

[§]Institut de Química Computacional i Catàlisi, Departament de Química, University of Girona, Campus de Montilivi sn, 17071 Girona, Catalonia, Spain

[‡]Department of Chemistry and Biology, University of Salerno, Via Ponte don Melillo, Fisciano I-84084, Italy

[‖]KAUST Catalyst Center, Physical Sciences and Engineering Division, King Abdullah University of Science and Technology, Thuwal 23955-6900, Saudi Arabia

ⓈSupporting Information

ABSTRACT: Olefin metathesis is a powerful tool for the formation of carbon–carbon double bonds. Several families of well-defined ruthenium (Ru) catalysts have been developed during the past 20 years; however, the reaction mechanism for all such complexes was assumed to be the same. In the present study, the initiation mechanism of Ru–indenylidene complexes was examined and compared with that of benzylidene counterparts. It was discovered that not all indenylidene complexes followed the same mechanism, highlighting the importance of steric and electronic properties of so-called spectator ligands, and that there is no single mechanism for the Ru-based olefin metathesis reaction. The experimental findings are supported quantitatively by DFT calculations.
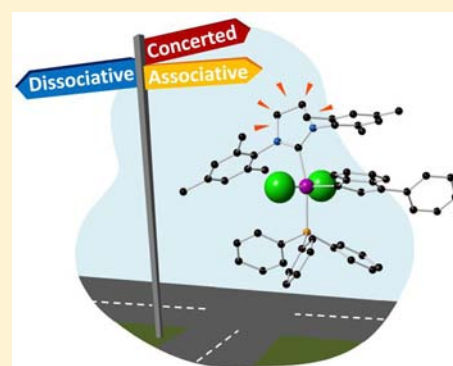
INTRODUCTION

Understanding the exact mechanism at play in the formation of any (or all) product(s) in the course of a chemical reaction is key to developing better catalysts.[1] The importance of reaction mechanisms is such that in the field of olefin metathesis, the clarification of the reaction sequence led to the 2005 Nobel Prize being awarded to Yves Chauvin shared with Richard Schrock and Robert Grubbs for his very insightful and meticulous mechanistic study.[2] Chauvin was the first to propose that the active catalyst was a metal–carbene complex and that a series of four-membered metallacycles led to the formation of the observed products.[2a,3] This discovery enabled the design of well-defined catalysts (Figure 1) and helped transform olefin metathesis into one of the most important tools for the formation of carbon–carbon bonds in modern synthetic chemistry.[4] This powerful synthetic tool renders accessible complex molecules that would be quite tedious to synthesize using traditional organic synthetic methods. As a testimony to its importance, metathesis reactions are now employed to access fine chemicals, biologically active compounds, new functionalized materials, and various polymers.[4d,f,5]

The accepted mechanism for olefin metathesis (using ring-closing metathesis, RCM, as a specific incarnation of the general reaction) of olefin metathesis first- and second-generation catalysts (**1a** and **2a**, respectively) can be divided
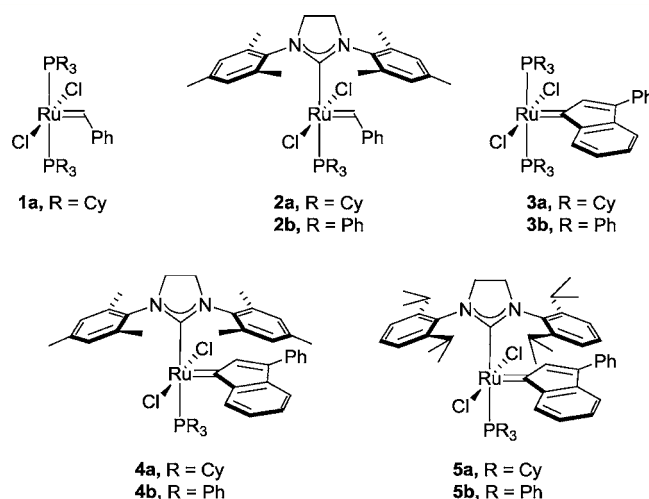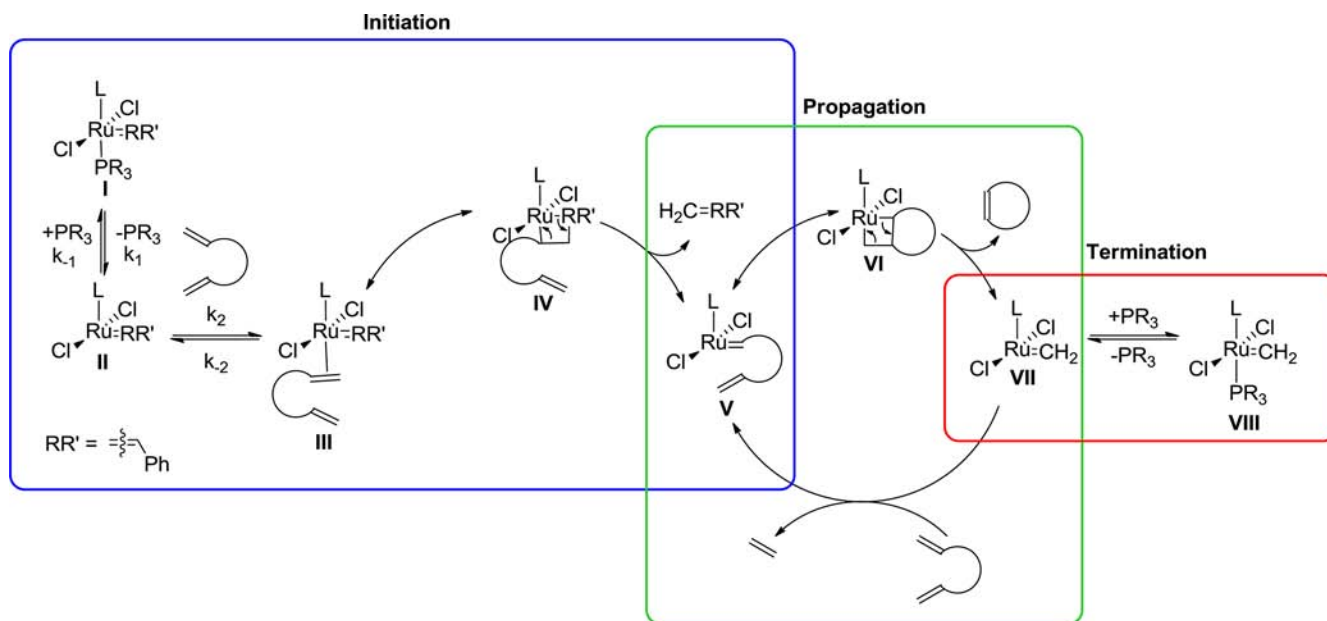

Figure 1. Ru complexes used in this study.

into three separate events: initiation, propagation, and termination (Scheme 1).[6]

Scheme 1. Accepted Mechanism of Olefin Metathesis with Grubbs-Type Catalysts

The first step of the accepted mechanism is the release of a tertiary phosphine (PR_3) from **I** to form a 14-electron species (**II**) that then coordinates the olefin. Formation of a metallacycle (**IV**) followed by rearrangement of the bonds to release the benzylidene moiety initially attached to the metal center leads to a new carbene (**V**).[7]

Subsequent coordination of the second double bond leads to the formation of the metallacycle (**VI**) that is rearranged to form the product and the propagating species [Ru(═CH$_2$)Cl$_2$L] (**VII**), which can react with further olefins and proceed along the catalytic cycle or react with a phosphine and form a resting species (**VIII**) that does not lead to any further catalytic turnovers.

A detailed study by Grubbs using magnetization transfer experiments to probe the first step of the mechanism revealed that there is a complex relationship between phosphine dissociation rates (k_1) and activity (see Scheme 1). First-generation catalysts (i.e., **1** and **3**) have higher phosphine dissociation rates than second-generation complexes (i.e., **2** and **4**), although second-generation catalysts are more active. It was shown that the difference in activity is due to the higher affinity of N-heterocyclic carbene (NHC)-containing catalysts for olefin over phosphine coordination. This can be rationalized in terms of a lower k_{-1}/k_2 ratio, which translates into more efficient initiation of the precatalysts. However, for second-generation catalysts a linear free energy relationship exists between phosphine σ-donor ability and the rate of catalyst initiation (phosphine dissociation), demonstrating that initiation could be controlled by tuning the phosphine electronic properties.[6c]

The initiation step in olefin metathesis has been the subject of recent debate.[8] While the mechanism for Ru first- and second-generation catalysts (**1a** and **2b**, respectively) has been studied in depth and is widely accepted, the mechanism for other families of catalyst has not until recently been studied in detail but has generally been assumed to be identical to that reported for **1a** and **2b**. Recent reports on the initiation of a different class of well-defined complexes, Hoveyda-type complexes, have shown that the preference for an associative/

interchange or a dissociative initiation mechanism in this family depends on the electronic and steric configuration of the complex and of the olefin studied.[8]

As precatalysts **1**−**5** all generate the same active species after one catalytic turnover, the main differences in reactivity between these complexes should be associated with the relative ease of the initiation step.[4h] In light of our recent reports describing several ruthenium (Ru)−indenylidene complexes,[9] we focused our attention on the activation mechanism of Ru−indenylidene complexes in olefin metathesis. Our goal was to understand the effects of electronic modifications on catalytic activity and to compare indenylidene complexes with their benzylidene counterparts to confirm (or not) whether the assumed generality of the mechanism held true.

■ RESULTS AND DISCUSSION

The overall reaction mechanism of olefin metathesis involves several intermediates that cannot be observed on the NMR time scale (Scheme 1). However, the first step of the proposed mechanism, the release of a phosphine to form the catalytically active species, can be studied using magnetization transfer experiments.[6] There are three possible pathways for the phosphine exchange process: dissociative, associative, and interchange (Scheme 2). In the dissociative pathway, the phosphine is released, forming a 14-electron species that can then coordinate to a new phosphine. In the associative pathway a new phosphine coordinates to the metal center forming an 18-electron intermediate followed by the release of one phosphine. In the interchange mechanism a new phosphine binds to the metal center, while the originally bound phosphine is simultaneously released (Scheme 2).

Grubbs measured the dissociation rate constant k_1 for several benzylidene catalysts by magnetization transfer experiments employing the delay alternating with nutation for tailored excitation (DANTE) pulse sequence, with postanalysis of the data by the nonlinear fit program CIFIT.[6] We have employed a novel and faster method utilizing selective 1D ^{31}P exchange spectroscopy (EXSY) instead.[10] (Note: All experiments performed with the new EXSY pulse sequence were done

Scheme 2. Possible Phosphine Exchange Pathways

A) Dissociative

B) Associative

C) Interchange
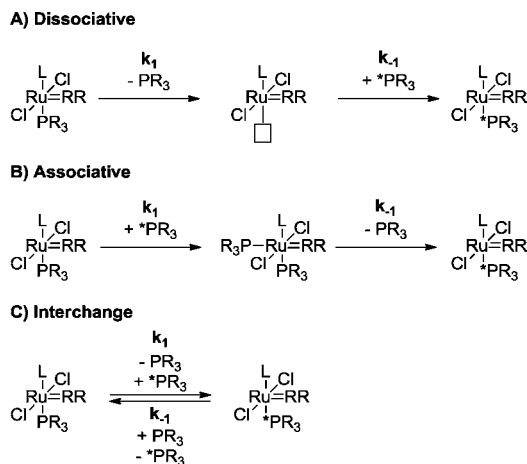
using the same concentrations as previously studied and reported by Grubbs; for this reason the values can be compared directly.) The activation parameters and the dissociation rate constant at 353 K for complexes **1**–**5** are presented in Table 1.

Table 1. Activation Parameters for Precatalysts 1a–5b

	cat.	$k_{1, 353 K}$ (s^{-1})	$\Delta H^{\ddagger}$ (kcal/mol)	$\Delta S^{\ddagger}$ (cal/K·mol)	$\Delta G^{\ddagger}_{298 K}$ (kcal/mol)
1	**1a**[b]	9.6	23.6(5)	12(2)	19.88(6)
2	**2a**[b]	0.13	27(2)	13(6)	23.0(4)
3	**2a**[c]	0.12	27(7)	12(19)	23(9)
4	**2a**	0.12	27(4)	12(10)	23(5)
5	**2b**[e]	7.5	21.9(4)	7(1)	19.7(4)
6	**3a**	1.72	23(1)	8(4)	21(2)
7	**3b**	236[d]	26(5)	26(18)	18(8)
8	**4a**	<0.01	nd	nd	nd
9	**4b**	0.19	17(3)	−13(8)	21(4)
10	**5b**	4.29	27(1)	21(4)	21(2)

[a]Values determined using $^{31}P\{^{1}H\}$ EXSY experiments; reaction conditions: [Ru] = 0.04 M in toluene-d_8 and 1.5 equiv of free phosphine. [b]Values obtained from ref 6b. [c]Values determined using the DANTE-CIFIT protocol. [d]Extrapolated using the Eyring equation; nd = not determined [e]Values obtained from ref 6c.

In order to validate the new method, k_1 for complex **2a** was determined using both methods and compared with the literature value. Excellent agreement between all three values was obtained (entries 2–4).

As expected, there is a significant difference in k_1 depending on the nature of the alkylidene moiety; overall, the exchange rate is significantly slower for indenylidene complexes compared to their benzylidene counterparts. In fact, the exchange constant for **4a** is so small that it could not be measured using this method. This agrees with the experimental finding that indenylidene complexes are more thermally stable than their benzylidene congeners, as catalyst decomposition is proportional to the amount of catalytically active species present in solution.[11]

Consistent with previous findings,[6b,c] changing from PPh_3 to PCy_3 dramatically increases the exchange rate. Surprisingly, $k_{1, 353 K}$ for metathesis inactive **3b** is over 100 times greater than for **3a** and so rapid that the exchange could be observed at room temperature, although the Ru complex is not metathesis-active.
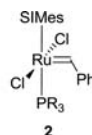
The most surprising result, among those presented in Table 1, was the negative value for the entropy of activation ($\Delta S^{\ddagger}$) for the phosphine exchange involving complex **4b**. This result strongly suggests that the exchange mechanism for this complex does not follow the "traditional" dissociative pathway; instead, an associative or interchange mechanism would be more consistent with such an entropy value.

In order to investigate this alternative mechanistic hypothesis, the influence of the phosphine concentration on the exchange rate (Table 2) in Ru complexes bearing different *para*-substituted triphenylphosphine was studied.
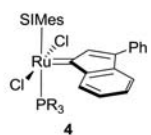
Grubbs reported that for second-generation benzylidene complexes, such as **2**, the exchange rate is independent of the concentration of phosphine.[6] This is not the observed situation for indenylidene complexes! Indeed, the phosphine exchange rate increases with the concentration of phosphine, further supporting the hypothesis of a different exchange mechanism in these complexes. Interestingly, the exchange rates for indenylidene complexes do not follow the trend $P(p$-$CH_3C_6H_4)_3$ < PPh_3 < $P(p$-$CF_3C_6H_4)_3$, suggesting that the electronic properties of the phosphines are not the sole factors influencing the reaction mechanism.

Changing the NHC also has an important effect on k_1. When complex **5a**, bearing the sterically demanding 1,3-bis(2,6-

Table 2. Exchange Rate (k_1) for Ru–Benzylidene and Ru–Indenylidene Complexes Bearing *para*-Substituted Triphenylphosphines at 353 K[a]


	k_1 for different equiv. of PR_3 (s^{-1})			
	Benzylidene (2)	Indenylidene (4)		
R	1.5[b]	1.5	5	10
c = (p-CH₃C₆H₄)	4.1	0.027	0.035	0.73
b = C₆H₅	7.5	0.19	0.32	1.25
d = (p-CF₃C₆H₄)	48	0.099	0.21	0.43

[a]Values determined using $^{31}P\{^{1}H\}$ EXSY experiments; reaction conditions: [Ru] = 0.04 M in toluene-d_8 and relative equivalents of free phosphine [b]Extracted from ref 6c.

diisopropylphenyl)-4,5-dihydroimidazol-2-ylidene (SIPr) ligand, is dissolved in a solution containing PCy$_3$, the complex reacts with the excess phosphine and forms the corresponding bis-PCy$_3$ complex **3a**. This result suggests that NHC dissociation is not as difficult as believed for the **SIPr** ligand and explains why complex **5a** has never been isolated in pure form from the reaction mixture of **3a** with free **SIPr**, as the exchange reaction is in reality an equilibrium (eq 1).[9b]
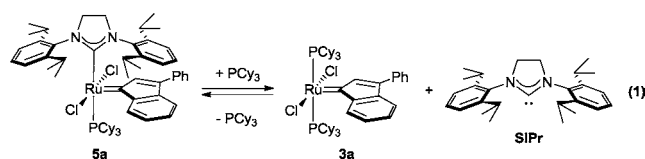

In addition to the different reactivity observed toward an excess of PCy$_3$, changing the NHC also has a profound effect on the initiation mechanism. Complex **5b** bearing a **SIPr** ligand exhibits a dissociative behavior confirmed by the high positive value of the entropy of activation compared to the negative value obtained for its 1,3-bis(2,4,6-trimethylphenyl)-4,5-dihydroimidazolin-2-ylidene (SIMes)-bearing relative **4b**. Interestingly $\Delta G^{\ddagger}$ is similar for both processes (Table 1).

In light of our previous findings, we next examined the reaction profile of **4b** with butyl vinyl ether (BVE). The reaction of catalysts with vinyl ethers is known to lead to catalytically inactive Fischer-type carbenes after a single turnover and provides a straightforward reaction with which to study the initiation kinetics without having to consider the propagation steps (Scheme 3).

Scheme 3. Possible Initiation Pathways of Olefin Metathesis Precatalysts with BVE
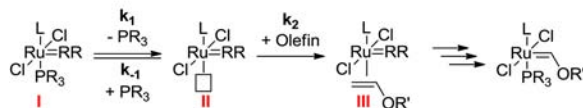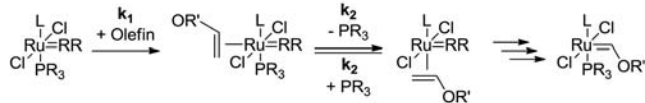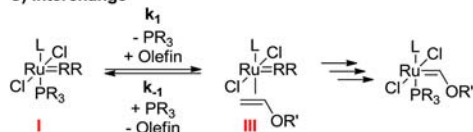

As observed in Table 3, there is a linear correlation between the concentration of BVE and the reaction rate for **4b** at the concentrations studied, while for **5b**, the reaction rate remains constant (within experimental error), thus again supporting the hypothesis of an associative or interchange mechanism of activation for complex **4b**.

It was previously reported by Grubbs that for first-generation catalysts the dissociation of the phosphine is not the rate-determining step for the reaction, and an almost linear correlation between the concentration of ethyl vinyl ether (EVE) and k_1 was observed for complexes with $k_1 > 1$ s^{-1}.[6b]

In the case of benzylidene complexes, this was still consistent with a dissociative mechanism because the values obtained for

Table 3. Influence of the Concentration of BVE on k_{obs} for 4b and 5b and Activation Parameters for the Reaction of 4b and 5b with BVE[a]

[BVE] (mol/L)	k_{obs} (s^{-1}) × 10^{-5}	
	4b[b]	5b[c]
0.90	4.3(1)	82(2)
1.80	6.2(1)	84(4)
2.58	10.6(2)	84(5)
$\Delta H^{\ddagger d}$ (kcal/mol)	19(3)	25(2)
$\Delta S^{\ddagger d}$ (cal/K·mol)	−12(9)	14(9)
$\Delta G^{\ddagger}_{298\ K}{}^{d}$ (kcal/mol)	23(4)	21(4)

[a]Determined by ^{31}P{^{1}H}NMR, reaction conditions: [Ru] = 0.0176 M in toluene-d_8. [b]$T = 283$ K. [c]$T = 288$ K. [d]Determined by ^{31}P{^{1}H}NMR; reaction conditions: [Ru] = 0.0176 M, [BVE] = 0.9 M.

k_1 were far below those predicted by magnetization transfer experiments. In the case of **4b**, direct comparison of k_1 values obtained by magnetization transfer experiments and by initiation kinetics is not possible, as both values depend on the concentration of the catalysts and the substrate (phosphine or BVE). However, it is possible to compare the activation thermodynamic parameters for both processes (see Table 3) and these are consistent, within experimental error, with those reported in Table 1.

Based on the results obtained thus far, we can conclude that the effective initiation mechanism in the case of **4b** follows a different pathway than that operative for its benzylidene counterpart and is very likely to be associative or interchange in nature.

DFT calculations were performed to shed light on the different mechanisms of initiation at play for **4b** and **5b**. For consistency, we extended the analysis to **2b** and **3b**. Based on the experimental evidence, we focused on the dissociative and on the interchange mechanisms (Figure 2), up to the substrate (methyl vinyl ether, MVE) coordination intermediate.

We first focus on the dissociative mechanism whose energetics and labeling scheme are reported in Figure 2. Dissociation of PPh$_3$ from the 16-electron species **I** requires 12.8−21.8 kcal/mol, and the first-generation catalyst **3b** displays the lowest affinity to retain the PPh$_3$ ligand,[12] with an energy demand of only 12.8 kcal/mol, while the highest PPh$_3$ affinity, 21.8 kcal/mol, is calculated for **4b**, which is 3.2 kcal/mol higher than for the **SIPr** system **5b**. This is reasonable considering the bulkiness of the *ortho*-^{i}Pr group of **SIPr**.[13]

The dissociation energy of PPh$_3$ in **2b-I** (14.2 kcal/mol) allows us to rationalize the effect of the alkylidene moiety on the dissociation of the labile ligand. The electron deficiency at the Ru center in the 14-electron species **2b-II** is alleviated by a favorable interaction of the metal with an aromatic hydrogen of the almost perfectly rotated benzylidene moiety, with a distance Ru···H = 2.81 Å, (see Figure 2). Rotation of the bulky indenylidene is prevented by the **SIMes** ligand in **4b-II**, which reduces the interaction of the indenylidene with the Ru center, as indicated by the longer Ru···H = 3.11 Å distance. The net consequence of the reduced Ru···H indenylidene interaction and of the overall higher deformation in the indenylidene 14-electron structures is the minor stability of the 14-electron species **4b-II** and **5b-II** relative to **2b-II**. This is geometrically illustrated by the larger NHC−Ru−alkylidene angle and by a slightly larger rotation of the NHC ligand from perfect alignment with the Ru−alkylidene bond in **4b-II** (Figure 2).
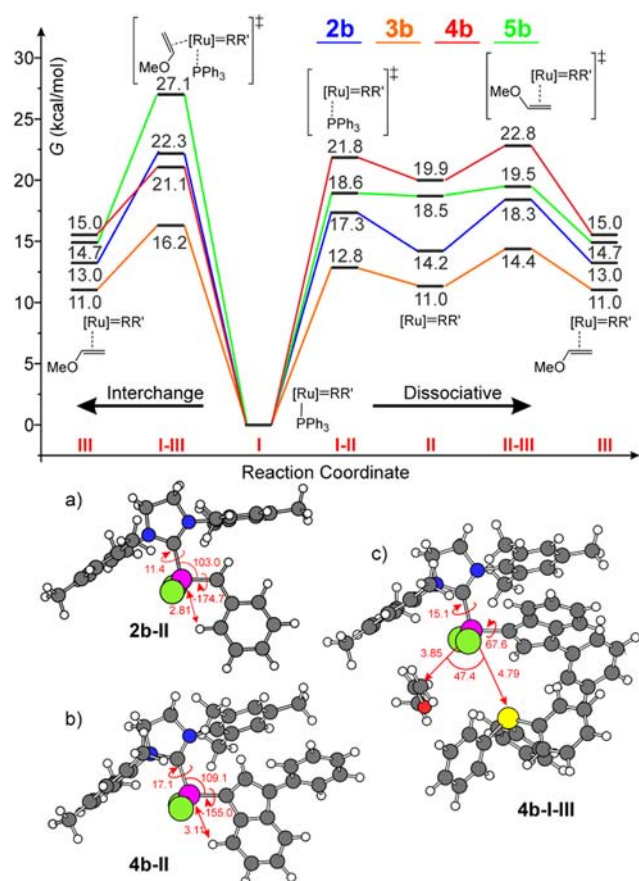
Figure 2. Free energy profile for initiation of **2b–5b** and main geometrical parameters of the 14-electron intermediates **2b-II** (a) and **4b-II** (b) and of the interchange transition state **4b-III** (c). Angles in deg (°), distances in Å.

The next step involves coordination of the olefin to **II**, with displacement of the aforementioned Ru···H interaction, to give the more stable coordination intermediate **III** through transition state **II–III**. For all systems, this is a rather facile step, the highest barrier being <5 kcal/mol, see Figure 2. Not surprisingly, the highest barrier is required for **2b-II** (4.1 kcal/mol) due to the stronger Ru···H interaction, while for **5b-II** this is almost a barrierless step, since the indenylidene moiety is nearly parallel to the aryl ring of the **SIPr** ligand (the *ortho* ^{i}Pr groups are very effective in blocking indenylidene rotation), and thus the incoming MVE is essentially free to engage with the Ru center without any spike in energy along the coordination pathway. Consistent with the above considerations, the MVE coordination intermediate **III** for systems with a NHC ligand is in the narrow window between 13.0 and 15.2 kcal/mol, since no Ru···H (alkylidene) interaction is present. Overall, the upper barrier for the dissociative initiation pathway, estimated as the energy difference between the highest in energy transition state **II–III** and the starting PPh$_3$ bound complex, ranges from 14.4 kcal/mol for system **3b** to 22.8 kcal/mol for system **4b** and reflects the stability of the 14-electron species **II**.

The metathesis events following **III** and leading to the metathesis inactive Fischer-type carbenes follow an energetically downhill trajectory occurring through classical steps described in a number of previous reports[14] (see Supporting Information). The only point we discuss here is the stability of the Ru–metallacycle formed by metathesis of MVE with the

Ru–alkylidene bond of **2b–5b**. This metallacycle is a relatively stable key intermediate of each metathesis event, and it has been characterized experimentally.[4g,7,15] Normally, the less substituted the metallacycle, the higher is its stability. According to our calculations, the metallacycle deriving from metathesis of MVE with **2b–5b** is 0.4, 8.4, 1.7, and 0.0 kcal/mol, respectively, higher in energy than the preceding coordination intermediate **III**, which immediately illuminates the difficulty of this coordination intermediate to evolve into the metallacycle for **3b**, thus explaining the poor catalytic performances of **3b**, whereas it is thermodynamically easily accessible for the NHC based catalysts **2b**, **4b**, and **5b**. Intrigued by this difference between first and second-generation systems, we examined the [RuCl$_2$(PCy$_3$)$_2$(indenylidene)] (**3a**) catalyst, since it is known that replacing PPh$_3$ by PCy$_3$ leads to active first-generation systems. Consistently, the metallacycle deriving from MVE metathesis with **3a** is only 0.4 kcal/mol above the preceding coordination intermediate, allowing us to suggest a possible relationship between the stability of the metallacycle intermediate and the potential catalytic activity of the corresponding Ru complex.

Characterization of the interchange initiation pathway requires finding the location of a single transition state, **I–III**, in which the entering MVE displaces a PPh$_3$ molecule still bound to the metal center, see Figure 2. The energy difference between transition state **I–III** and the starting PPh$_3$ bound complex immediately offers the energy barrier for the interchange pathway. The lower barrier, 16.2 kcal/mol, is calculated for **3b**, which is still consistent with the relatively low binding energy of PPh$_3$ in **3b**. As for the NHC-based systems, the barrier for **2b** and **4b**, around 21–22 kcal/mol, is significantly lower than the one calculated for **5b** (27.5 kcal/mol). This difference between **2b** and **4b** on the one side, and **5b** on the other, can be clearly ascribed to the bulkiness of the *ortho* ^{i}Pr groups of **5b**, which prevents the approach of other ligands to the metal center if the labile PPh$_3$ ligand is not first dissociated. In all **I–III** transition states, MVE approaches the metal center from the side of the vacant coordination position *trans* to the Ru–alkylidene bond. The **I–III** transition state for **4b** is presented in Figure 2 and shows that MVE approaches the metal along the only route allowed for an external ligand, which is *trans* to the Ru–alkylidene bond. The PPh$_3$ ligand is almost completely dissociated from the metal center, which is understandable, considering the small MVE–Ru–PPh$_3$ angle. Larger values for this angle are impossible due to the shielding of the above mesityl ring on the Ru vacant coordination position.[13a,16]

At this point, it is possible to compare the calculated energy barriers of the dissociative and the interchange pathways. According to the values reported in Figure 2, the dissociative pathway is favored for **2b**, **3b**, and **5b**, by 4.0, 1.8, and 7.5 kcal/mol, respectively, whereas the interchange pathway is favored for **4b** by 1.7 kcal/mol. Focusing on **4b** and **5b**, this conclusion is in qualitative agreement with the experimental results of Table 3. Furthermore, the calculated barriers for **4b** and **5b**, 21.1 and 20.0 kcal/mol, respectively, are in good quantitative agreement with the experimental values.

Having achieved a good agreement with the experiments allowed us to draw general conclusions and rationalize the activation mechanisms with NHC-based systems. Basically, the dissociative mechanism is favored by two factors: (1) a flexible alkylidene moiety, such as the benzylidene group, that allows to decrease the electron deficiency at the metal center, reducing

the energy cost required to form the 14-electron species. In this architecture, the stabilizing Ru···H (alkylidene) interaction we evidenced in **2b-II** is reminiscent of the much stronger Ru···O interaction in complexes presenting a chelating alkoxy-alkylidene group and (2) NHC ligands with bulky *ortho*-substituents, which prevent the approach of the substrate to the metal if a bulky labile ligand, such as PPh$_3$, is still coordinated to the metal. Here we remark that the average bulkiness of the SIMes and SIPr ligands, as estimated by the $\%V_{Bur}$, is approximately the same,[13] but the steric map of the two systems clearly indicates that SIPr is able to exert higher steric pressure than SIMes at the border of the first-coordination sphere around the metal,[13a] thus disfavoring the interchange mechanism.

The interchange mechanism is instead favored when a balance between electronic and steric effects is reached. More specifically, this mechanistic scenario is preferred if bulky and/or rigid alkylidene moieties, such as the indenylidene group, cannot engage effectively with the metal center to stabilize the 14-electron species and the NHC ligand is not bulky enough to prevent the approach of the substrate at the metal with the bulky PPh$_3$ still coordinated.

As a final remark, we note that the preference for one mechanism over the other is not very large. For **2b–4b** the disfavored activation pathway is <5 kcal/mol higher in energy than the favored pathway despite the mechanistic differences, which lead us to believe that small changes in the systems, substrates, and conditions can push the balance toward one or the other of the two activations pathways. This conclusion is in qualitative agreement with the complex experimental activation behavior evidenced in this work and in the competition between the dissociative and the interchange/associative mechanisms evidenced by Plenio and co-workers.[8a]

■ ASSOCIATED CONTENT

Ⓢ Supporting Information

Full experimental details as well as detailed information regarding the $\%V_{Bur}$ calculations, computational details, Cartesian coordinates and energies of all the species discussed in this work. The CIF files of crystal structures for **3a** and **4b** have been deposited in the CCDC no 887968 and 887969, respectively, these data can be obtained free of charge on applications to CCDC. This material is available free of charge via the Internet at http://pubs.acs.org.

■ AUTHOR INFORMATION

Corresponding Author

snolan@st-andrews.ac.uk; luigi.cavallo@kaust.edu.sa

Notes

The authors declare no competing financial interest.

■ ACKNOWLEDGMENTS

■ REFERENCES

(1) Poli, R. *Comments Inorg. Chem.* **2009**, *30*, 177−228.
(2) (a) Chauvin, Y. *Angew. Chem., Int. Ed.* **2006**, *45*, 3740−3747. (b) Grubbs, R. H. *Angew. Chem., Int. Ed.* **2006**, *45*, 3760−3765. (c) Schrock, R. R. *Angew. Chem., Int. Ed.* **2006**, *45*, 3748−3759.
(3) Herisson, J. L.; Chauvin, Y. *Makromol. Chem.* **1970**, *141*, 161−176.
(4) (a) Grubbs, R. H. *Handbook of Metathesis*; Wiley-VCH: Weinheim, Germany, 2003; Vol. *1−3*; (b) Nolan, S. P.; Boeda, F.; Clavier, H. *Chem. Commun.* **2008**, 2726−2740. (c) Samojłowicz, C.; Bieniek, M.; Grela, K. *Chem. Rev.* **2009**, *109*, 3708−3742. (d) Deiters, A.; Martin, S. F. *Chem. Rev.* **2004**, *104*, 2199−2238. (e) Lozano-Vila, A. M.; Monsaert, S.; Bajek, A.; Verpoort, F. *Chem. Rev.* **2010**, *110*, 4865−4909. (f) McReynolds, M. D.; Dougherty, J. M.; Hanson, P. R. *Chem. Rev.* **2004**, *104*, 2239−2258. (g) Vougioukalakis, G. C.; Grubbs, R. H. *Chem. Rev.* **2009**, *110*, 1746−1787. (h) Boeda, F.; Clavier, H.; Nolan, S. P. *Chem. Commun.* **2008**, 2726−2740.
(5) (a) Nicolaou, K. C.; Bulger, P. G.; Sarlah, D. *Angew. Chem., Int. Ed.* **2005**, *44*, 4490−4527. (b) Van de Weghe, P.; Eustache, J. *Curr. Top. Med. Chem.* **2005**, *5*, 1495−1519. (c) Donohoe, T. J.; Orr, A. J.; Bingham, M. *Angew. Chem., Int. Ed.* **2006**, *45*, 2664−2670. (d) Gradillas, A.; Perez-Castells, J. *Angew. Chem., Int. Ed.* **2006**, *45*, 6086−6101. (e) Compain, P. *Adv. Synth. Catal.* **2007**, *349*, 1829−1846. (f) Hoveyda, A. H.; Zhugralin, A. R. *Nature* **2007**, *450*, 243−251. (g) Kotha, S.; Lahiri, K. *Synlett* **2007**, *2007*, 2767−2784.
(6) (a) Sanford, M. S.; Ulman, M.; Grubbs, R. H. *J. Am. Chem. Soc.* **2001**, *123*, 749−750. (b) Sanford, M. S.; Love, J. A.; Grubbs, R. H. *J. Am. Chem. Soc.* **2001**, *123*, 6543−6554. (c) Love, J. A.; Sanford, M. S.; Day, M. W.; Grubbs, R. H. *J. Am. Chem. Soc.* **2003**, *125*, 10103−10109.
(7) van der EideEdwin, F.; Piers, W. E. *Nat. Chem.* **2010**, *2*, 571−576.
(8) (a) Thiel, V.; Hendann, M.; Wannowius, K.-J.; Plenio, H. *J. Am. Chem. Soc.* **2011**, *134*, 1104−1114. (b) Vorfalt, T.; Wannowius, K. J.; Thiel, V.; Plenio, H. *Chem.—Eur. J.* **2010**, *16*, 12312−12315. (c) Ashworth, I. W.; Hillier, I. H.; Nelson, D. J.; Percy, J. M.; Vincent, M. A. *Chem. Commun.* **2011**, *17*, 13087−13094.
(9) (a) Broggi, J.; Urbina-Blanco, C. A.; Clavier, H.; Leitgeb, A.; Slugovc, C.; Slawin, A. M. Z.; Nolan, S. P. *Chem.—Eur. J.* **2010**, *16*, 9215−9225. (b) Clavier, H.; Urbina-Blanco, C. A.; Nolan, S. P. *Organometallics* **2009**, *28*, 2848−2854. (c) Urbina-Blanco, C. A.; Bantreil, X.; Clavier, H.; Slawin, A. M. Z.; Nolan, S. P. *Beilstein J Org Chem* **2010**, *6*, 1120−1126. (d) Urbina-Blanco, C. A.; Leitgeb, A.; Slugovc, C.; Bantreil, X.; Clavier, H.; Slawin, A. M. Z.; Nolan, S. P. *Chem.—Eur. J.* **2011**, *17*, 5045−5053. (e) Urbina-Blanco, C. A.; Manzini, S.; Gomes, J. P.; Doppiu, A.; Nolan, S. P. *Chem. Commun.* **2011**, *47*, 5022−5024.
(10) (a) Kessler, H.; Oschkinat, H.; Griesinger, C.; Bermel, W. *J. Magn. Reson. (1969−1992)* **1986**, *70*, 106−133. (b) Bauer, C.; Freeman, R.; Frenkiel, T.; Keeler, J.; Shaka, A. J. *J. Magn. Reson. (1969−1992)* **1984**, *58*, 442−457.
(11) Hong, S. H.; Wenzel, A. G.; Salguero, T. T.; Day, M. W.; Grubbs, R. H. *J. Am. Chem. Soc.* **2007**, *129*, 7961−7968.
(12) Yang, H.-C.; Huang, Y.-C.; Lan, Y.-K.; Luh, T.-Y.; Zhao, Y.; Truhlar, D. G. *Organometallics* **2011**, *30*, 4196−4200.
(13) (a) Ragone, F.; Poater, A.; Cavallo, L. *J. Am. Chem. Soc.* **2010**, *132*, 4249−4258. (b) Poater, A.; Cosenza, B.; Correa, A.; Giudice, S.; Ragone, F.; Scarano, V.; Cavallo, L. *Eur. J. Inorg. Chem.* **2009**, *2009*, 1759−1766.
(14) (a) Poater, A.; Ragone, F.; Correa, A.; Cavallo, L. *Dalton Trans.* **2011**, *40*, 11066−11069. (b) Credendino, R.; Poater, A.; Ragone, F.; Cavallo, L. *Catal. Sci. Technol.* **2011**, *1*, 1287−1297.

(15) (a) Rowley, C. N.; van der Eide, E. F.; Piers, W. E.; Woo, T. K. *Organometallics* **2008**, *27*, 6043−6045. (b) Romero, P. E.; Piers, W. E. *J. Am. Chem. Soc.* **2007**, *129*, 1698−1704. (c) van der Eide, E. F.; Romero, P. E.; Piers, W. E. *J. Am. Chem. Soc.* **2008**, *130*, 4485−4491.

(16) Poater, A.; Ragone, F.; Correa, A.; Cavallo, L. *J. Am. Chem. Soc.* **2009**, *131*, 9000−9006.